

Quantum dots enhanced Cerenkov luminescence imaging

Chang-Ran Geng^{1,2} · Yao Ai^{1,2} · Xiao-Bin Tang^{1,2} · Di-Yun Shu^{1,2} · Chun-Hui Gong^{1,2} · Ming-Hua Du³ · Fa-Quan Ji³

Received: 4 September 2018 / Revised: 22 December 2018 / Accepted: 3 January 2019 / Published online: 9 April 2019
© China Science Publishing & Media Ltd. (Science Press), Shanghai Institute of Applied Physics, the Chinese Academy of Sciences, Chinese Nuclear Society and Springer Nature Singapore Pte Ltd. 2019

Abstract Cerenkov luminescence imaging (CLI) has been widely investigated for biological imaging. However, the luminescence generated from Cerenkov effect is relatively weak and has poor penetration ability in biological tissues. These limitations consequently hindered the clinical translation of CLI. In this study, we proposed an in vitro experimental study for the demonstration of quantum dots (QDs) configurations affected by the improvement of the signal intensity of CLI. Results revealed that the optimal concentrations were 0.1 mg/mL and 0.25 mg/mL for the studied CdSe/ZnS QDs with fluorescence emission peaks of 580 nm and 660 nm, respectively. The detected optical signal intensity with long-wavelength emission QDs were stronger than those with short-wavelength emission QDs. This study illustrates an experiment to study the effects of

concentrations and fluorescence emission peaks of QDs on an enhanced optical signal for the external detection of CLI.

Keywords Cerenkov luminescence imaging · Quantum dots · Optical signal · Wavelength shift

1 Introduction

Cerenkov luminescence imaging (CLI) is a promising technique for advanced biology imaging in the medical field [1–5]. The application of CLI has been extended to determine tumor location [6, 7], monitor radionuclide uptake [8, 9], and guide tumor resection surgery [10, 11]. According to Frank and Tamm's theory, the wavelength of Cerenkov luminescence (CL) is mostly distributed in the ultraviolet and blue range, which can only penetrate a few millimeters of biological tissues owing to high attenuation coefficients, thereby limiting the application of CLI.

To overcome these limitations, several studies have been performed to explore novel technologies that can efficiently detect the signal, e.g., the CL endoscopy system [12–14]. Another potential solution is to shift the peak wavelength of CL to near-infrared or infrared ranges that have smaller attenuation coefficients. Cerenkov energy transfer (CRET) has demonstrated that CL can serve as an excitation source to excite various fluorescent particles, such as quantum dots (QDs) [15, 16], gold nanoparticles [17, 18], fluorophores [19], and lanthanides [20, 21], where the fluorescent particles can act as fluorescence emitters of red-shifted emissions. Near-infrared or infrared light has lesser attenuation and absorption by biological tissues than ultraviolet or blue light [22].

This work was supported in part by the Natural Science Foundation of Jiangsu Province (No. BK20180415), the National Natural Science Foundation of China (No. 11805100), the Fundamental Research Funds for the Central Universities (No. NS2018041), and the National Key Research and Development Program (Nos. 2016YFE0103600 and 2017YFC0107700).

Chang-Ran Geng and Yao Ai have contributed equally to this work.

✉ Xiao-Bin Tang
tangxiaobin@nuaa.edu.cn

¹ Department of Nuclear Science and Engineering, Nanjing University of Aeronautics and Astronautics, Nanjing 210016, China

² Collaborative Innovation Center of Radiation Medicine of Jiangsu Higher Education Institutions, Nanjing 210016, China

³ Affiliated Hospital of Nanjing University of TCM, Nanjing 210016, China

Among various fluorescent particles, QDs were proposed to be combined with radioisotopes to construct CRET systems because QDs have superior optical properties, such as large Stokes shift, tunable fluorescence emission, high photostability, and high quantum yield [23–25]. However, whether high concentrations of QDs coupled with radioisotopes enhance optical signals for external detection still remains unclear. Appropriate fluorescence wavelength emissions of QDs can be selected for better optical signal enhancements considering the various penetrating abilities and quantum efficiencies of different photonic wavelengths of the external optical detector. In this study, two types of core/shell QDs (i.e., CdSe/ZnS and CdTe/CdS) were selected to evaluate the effects of the concentration and fluorescence emission peaks of QDs on optical signal enhancement for external detection.

2 Experiments section

CdSe/ZnS and CdTe/CdS core/shell QDs were obtained from Xingzi New Material Technology Development Co. Ltd. (Shanghai, China). The fluorescence emission peaks were 580 nm and 660 nm for CdSe/ZnS QDs, and 580 nm and 620 nm for the CdTe/CdS QDs. Experiments were performed on an in-house developed optical imaging platform (see Fig. 1a), which was mainly composed by an EMCCD camera inside a black box to minimize the distortion of background light. The distance between the lens of the EMCCD and the transparent vials was 35 cm. The Na¹³¹I/QD mixed solution and the Na¹³¹I solution were imaged on the top of the sample. All images were acquired with a 4 × 4 binning and a 5-min exposure time. The areas of the regions of interest were drawn over the optical sources of the images, and the average number of photons was calculated with Andor Solis that was used to provide the quantification information from the optical images. To

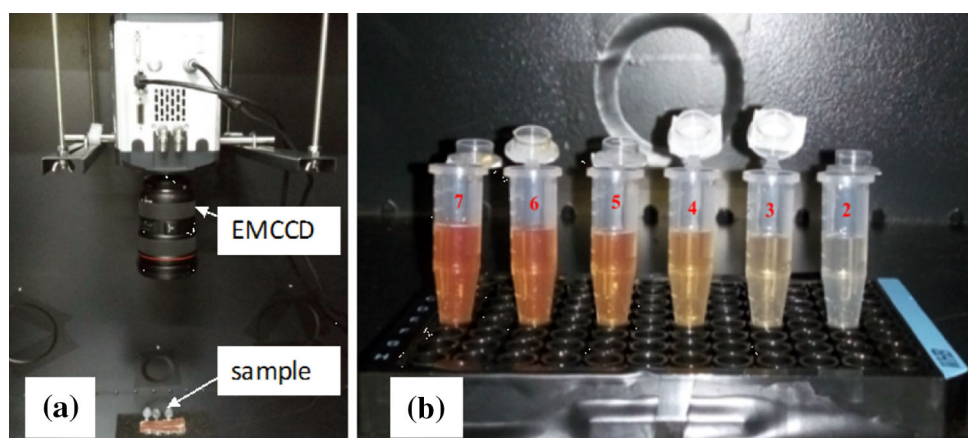
evaluate the enhancement effect of QDs on optical signals for the Na¹³¹I solution, QDs with different fluorescence emission peaks (1 mL) were prepared in transparent vials with various concentrations (i.e., 0.05, 0.1, 0.25, 0.5, 0.75, and 1 mg/mL) as shown in Fig. 1b. The control group was prepared with zero QDs. Thereafter, 30 and 60 μCi Na¹³¹I (0.5 mL) solutions were added to each transparent vial, respectively.

To study the enhancement effect of QDs on the transmission ability in muscle tissues, a soft tissue of a pig was put on top of the vials. Figure 2 shows the experimental setup that was illustrated through the optical image of the muscle tissue covering the transparent vials. Different concentrations of CdTe/CdS QDs with 60 μCi of Na¹³¹I were placed in the transparent vials at 620 nm. The enhancement effect on the optical signal was related to the concentration of QDs for the same Na¹³¹I radioactivity.

3 Results and discussion

Figure 3 shows the optical images of different concentrations of CdTe/CdS QDs added with Na¹³¹I (60 μCi) solution at 620 nm. The signal intensity increases as the concentration of the QDs increases up to 0.75 mg/mL, and decreases as the concentration of the QDs further increases. The two types of QDs showed similar patterns. Figure 4a, b shows the total number of photons at fluorescence emission peaks of 580 nm and 660 nm for the CdSe/ZnS QDs added with Na¹³¹I solution (30 and 60 μCi), and for CdTe/CdS QDs, respectively. This phenomenon may be due to the concentration quenching effect [26] that occurs when the concentration of QDs is excessively high, while the excitation intensity remains unchanged [27]. Alternatively, the self-absorption of the solution is another factor that decreases the photons. Different kinds and emission peaks of QDs have different optimal concentrations to enhance

Fig. 1 (Color online)
a Experimental setup of the EMCCD system and **b** prepared QDs solutions



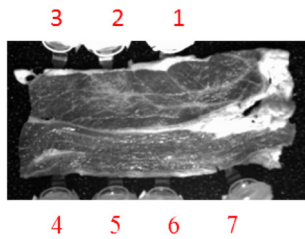


Fig. 2 Experimental setup for the transmission study that was designed with the soft tissue of pig sitting on top of the prepared solutions

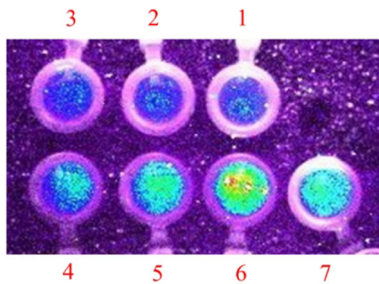


Fig. 3 (Color online) Optical image of the Na¹³¹I/quantum dot mixed solution

the signal intensity of the Na¹³¹I solution. The optimal concentrations of CdSe/ZnS at fluorescence emission peaks of 580 nm and 660 nm were 0.1 mg/mL and 0.25 mg/mL, respectively. By comparison, the optimal concentrations of CdTe/CdS at fluorescence emission peaks of 580 nm and

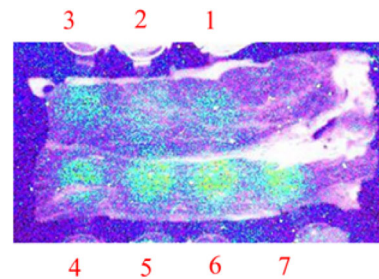


Fig. 5 (Color online) Optical image of muscle tissue covering transparent vials

620 nm were 0.1 and 0.75 mg/mL, respectively. Moreover, the number of photons in all mixed solutions was greater than that of the pure Na¹³¹I solution exposed to the same radioactivity level, suggesting that QDs successfully converted CL into red-shifted photons, which has higher penetration ability in tissues.

Figure 5 shows the imaging of photons that are transmitted through the soft tissue. Figure 6a, b shows the results for CdTe/CdS QDs added with 60 μCi of Na¹³¹I solution. Under these conditions, the number of photons decreases as the thickness of the muscle tissue increases; however, it was always greater than that of the pure Na¹³¹I solution with the same radioactivity level. These results indicated that the QDs successfully converted CL into red-shifted photons that could enhance the penetration ability of photons in tissues. The spatial distribution of the tissue

Fig. 4 Scatter plot of the number of photons at fluorescence emission peaks of **a** 580 nm and **b** 660 nm for the CdSe/ZnS QDs, and **c** 580 nm and **d** 620 nm for the CdTe/CdS QDs with Na¹³¹I solution

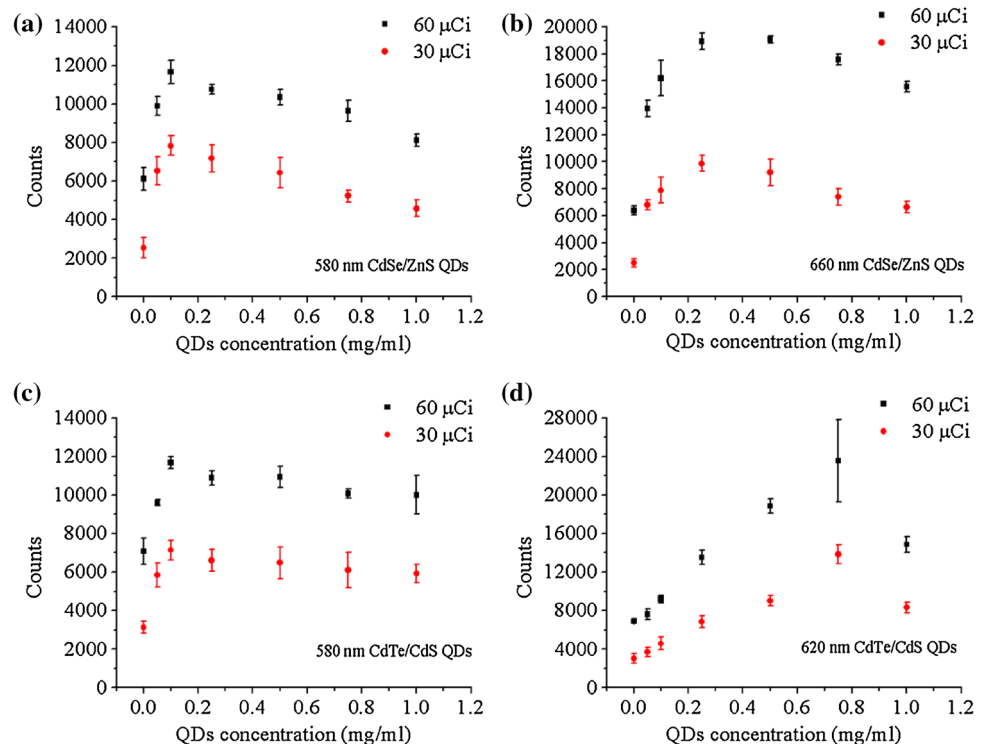


Fig. 6 Scatter plot of optical signals that were detected by the EMCCD with different concentrations of CdTe/CdS QDs added with 60 μCi of Na^{131}I solution and covered with muscle tissues of varying thicknesses at fluorescence emission peaks of **a** 580 nm and **b** 660 nm

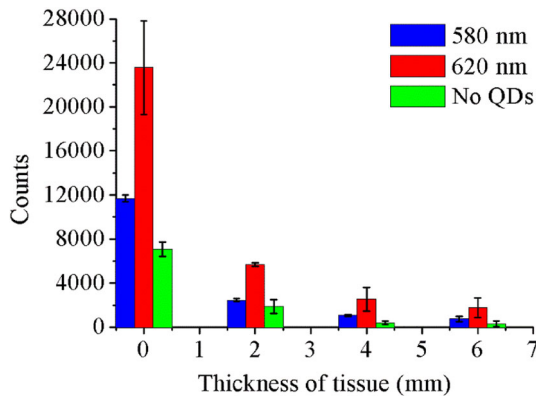
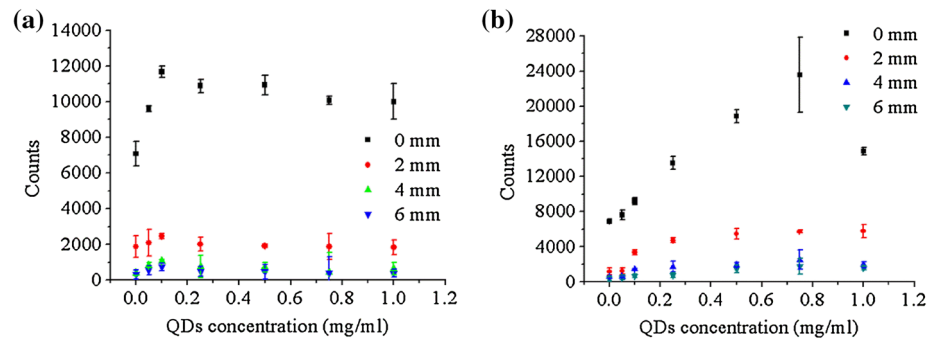


Fig. 7 (Color online) Total number of photons at the optimal concentrations of CdTe/CdS QDs added with 60 μCi of Na^{131}I solution and covered with muscle tissues of different thicknesses

optical properties is indeed heterogeneous considering the whole sample; however, in our experiment, we attempt to determine a relatively uniform area for experiment that intentionally avoids the effect from the sample heterogeneity. Figure 7 shows the total number of photons at optimal concentrations of CdTe/CdS QDs added with 60 μCi of Na^{131}I solution and covered with muscle tissues of different thicknesses. For the same type of QDs, the attenuation of the number of photons at the fluorescence emission peaks of short-wavelength emission QDs was more severe than that of long-wavelength emission QDs. Therefore, the fluorescence emission peaks of the long-wavelength emission QDs were more suitable for the enhancement of optical signal intensity for external detection than those of the short-wavelength emission QDs. This result is consistent with the previous studies on the in vitro animal studies and optical properties of biological tissues, which generally show lower absorption efficiencies for longer-wavelength emission QDs [15, 28, 29]. To further explore the underlying mechanisms, the percentage of Cherenkov light that is being converted to longer-wavelength photons could be explored through spectroscopic studies.

4 Conclusion

In this study, we experimentally observed the enhancement effect of CdSe/ZnS and CdTe/CdS QDs on optical signals that may be detected by an external optical detector (e.g. EMCCD) for CLI. The results indicated that QDs could effectively enhance the optical signal that could be detected by an external EMCCD, and different types and emission peaks of QDs have different patterns (e.g. various optimal concentrations) on the enhancement of the signal intensity of CL for external detection. For the same type of QDs, the long-wavelength emission QDs were more suitable than short-wavelength emission QDs for the improvement of optical signal intensity.

References

1. A.E. Spinelli, D. D'Ambrosio, L. Calderan et al., Cherenkov radiation allows in vivo optical imaging of positron emitting radiotracers. *Phys. Med. Biol.* **55**, 483 (2009). <https://doi.org/10.1088/0031-9155/55/2/010>
2. B. Brichard, A. Fernandez, H. Ooms et al., Fibre-optic gamma-flux monitoring in a fission reactor by means of Cherenkov radiation. *Meas. Sci. Technol.* **18**, 3257 (2007). <https://doi.org/10.1088/0957-0233/18/10/S32>
3. J.S. Cho, R. Taschereau, S. Olma et al., Cherenkov radiation imaging as a method for quantitative measurements of beta particles in a microfluidic chip. *Phys. Med. Biol.* **54**, 6757 (2009). <https://doi.org/10.1088/0031-9155/54/22/001>
4. A.K. Glaser, J.M. Andreozzi, S.C. Davis et al., Video-rate optical dosimetry and dynamic visualization of IMRT and VMAT treatment plans in water using Cherenkov radiation. *Med. Phys.* (2014). <https://doi.org/10.1118/1.4875704>
5. R. Robertson, M.S. Germanos, C. Li et al., Optical imaging of Cherenkov light generation from positron-emitting radiotracers. *Phys. Med. Biol.* **54**, N355 (2009). <https://doi.org/10.1088/0031-9155/54/16/N01>
6. S.K. Pandey, J. Kaur, B. Easwaramoorthy et al., Multimodality imaging probe for positron emission tomography and fluorescence imaging studies. *Mol. Imaging* **13**, 7290-2014 (2014). <https://doi.org/10.2310/7290.2014.00005>
7. Y. Zhang, H. Hong, J.W. Engle et al., Positron emission tomography and optical imaging of tumor CD105 expression with a dual-labeled monoclonal antibody. *Mol. Pharm.* **9**, 645-653 (2012). <https://doi.org/10.1021/mp200592m>

8. Z. Hu, X. Ma, X. Qu et al., Three-dimensional noninvasive monitoring iodine-131 uptake in the thyroid using a modified Cerenkov luminescence tomography approach. *PLoS ONE* **7**, e37623 (2012). <https://doi.org/10.1371/journal.pone.0037623>
9. M. Nahrendorf, E. Keliher, B. Marinelli et al., Hybrid PET-optical imaging using targeted probes. *Proc. Natl. Acad. Sci. USA* **107**, 7910–7915 (2010). <https://doi.org/10.1073/pnas.0915163107>
10. C. Gigliotti, L. Altabella, F. Boschi et al., Monte Carlo feasibility study for image guided surgery: from direct beta minus detection to Cerenkov luminescence imaging. *J. Instrum.* **11**, P07021 (2016). <https://doi.org/10.1088/1748-0221/11/07/P07021>
11. J.S. Klein, G.S. Mitchell, S.R. Cherry, Quantitative assessment of Cerenkov luminescence for radioguided brain tumor resection surgery. *Phys. Med. Biol.* **62**, 4183 (2017). <https://doi.org/10.1088/1361-6560/aa6641>
12. C.M. Carpenter, X. Ma, H. Liu et al., Cerenkov luminescence endoscopy: improved molecular sensitivity with β^- -emitting radiotracers. *J. Nucl. Med.* **55**, 1905 (2014). <https://doi.org/10.2967/jnumed.114.139105>
13. S.-R. Kothapalli, H. Liu, J.C. Liao et al., Endoscopic imaging of Cerenkov luminescence. *Biomed. Opt. Express* **3**, 1215–1225 (2012). <https://doi.org/10.1364/BOE.3.001215>
14. H. Liu, C.M. Carpenter, H. Jiang et al., Intraoperative imaging of tumors using Cerenkov luminescence endoscopy: a feasibility experimental study. *J. Nucl. Med.* **53**, 1579 (2012). <https://doi.org/10.2967/jnumed.111.098541>
15. R.S. Dothager, R.J. Goiffon, E. Jackson et al., Cerenkov radiation energy transfer (CRET) imaging: a novel method for optical imaging of PET isotopes in biological systems. *PLoS ONE* **5**, e13300 (2010). <https://doi.org/10.1371/journal.pone.0013300>
16. J. Li, L.W. Dobrucki, M. Marjanovic et al., Enhancement and wavelength-shifted emission of Cerenkov luminescence using multifunctional microspheres. *Phys. Med. Biol.* **60**, 727 (2015). <https://doi.org/10.1088/0031-9155/60/2/727>
17. O. Volotskova, C. Sun, J.H. Stafford et al., Efficient radioisotope energy transfer by gold nanoclusters for molecular imaging. *Small* **11**, 4002–4008 (2015). <https://doi.org/10.1002/sml.201500907>
18. C. Zhou, G. Hao, P. Thomas et al., Near-infrared emitting radioactive gold nanoparticles with molecular pharmacokinetics. *Angew. Chem.* **124**, 10265–10269 (2012). <https://doi.org/10.1002/anie.201203031>
19. Y. Bernhard, B. Collin, R.A. Decréau, Inter/intramolecular Cerenkov radiation energy transfer (CRET) from a fluorophore with a built-in radionuclide. *Chem. Commun.* **50**, 6711–6713 (2014). <https://doi.org/10.1039/c4cc01690d>
20. X. Cao, X. Chen, F. Kang et al., Intensity enhanced Cerenkov luminescence imaging using terbium-doped Gd₂O₃ microparticles. *ACS. Appl. Mater. Interfaces* **7**, 11775–11782 (2015). <https://doi.org/10.1021/acsami.5b00432>
21. X. Ma, F. Kang, F. Xu et al., Enhancement of Cerenkov luminescence imaging by dual excitation of Er³⁺, Yb³⁺-doped rare-earth microparticles. *PLoS ONE* **8**, e77926 (2013). <https://doi.org/10.1371/journal.pone.0077926>
22. D.L. Thorek, A. Ogirala, B.J. Beattie et al., Quantitative imaging of disease signatures through radioactive decay signal conversion. *Nat. Med.* **19**, 1345 (2013). <https://doi.org/10.1038/nm.3323>
23. F. Boschi, A.E. Spinelli, Quantum dots excitation using pure beta minus radioisotopes emitting Cerenkov radiation. *RSC Adv.* **2**, 11049–11052 (2012). <https://doi.org/10.1039/c2ra22101b>
24. X. Michalet, F. Pinaud, L. Bentolila et al., Quantum dots for live cells, in vivo imaging, and diagnostics. *Science* **307**, 538–544 (2005). <https://doi.org/10.1126/science.1104274>
25. X. Tang, X. Hou, D. Shu et al., Research on the interaction mechanism between quantum dots and radionuclides for the improvement of Cerenkov luminescence imaging. *Sci. China Technol. Sci.* **58**, 1712–1716 (2015). <https://doi.org/10.1007/s11431-015-5897-x>
26. S. Rempel, A. Podkorytova, A. Rempel, Concentration quenching of fluorescence of colloid quantum dots of cadmium sulfide. *Phys. Solid State* **56**, 568–571 (2014). <https://doi.org/10.1134/S1063783414030251>
27. D.M. Willard, L.L. Carillo, J. Jung et al., CdSe–ZnS quantum dots as resonance energy transfer donors in a model protein–protein binding assay. *Nano Lett.* **1**, 469–474 (2001). <https://doi.org/10.1021/nl015565n>
28. S.L. Jacques, Optical properties of biological tissues: a review. *Phys. Med. Biol.* **58**, R37 (2013). <https://doi.org/10.1088/0031-9155/58/11/R37>
29. K. Kwon, T. Son, K.-J. Lee et al., Enhancement of light propagation depth in skin: cross-validation of mathematical modeling methods. *Lasers Med. Sci.* **24**, 605–615 (2009). <https://doi.org/10.1007/s10103-008-0625-4>